Ferromagnetic quantum singularities and small pseudogap formation in Heusler type $Fe_{2+x}V_{1-x}Al$

T. Naka,[1,*] K. Sato,[1] M. Taguchi,[1] T. Nakane,[1] F. Ishikawa,[2] Yuh Yamada,[3] Y. Takaesu,[4] T. Nakama,[4] and A. Matsushita[1]
[1]*National Institute for Materials Science, Tsukuba, Sengen 1-2-1, Tsukuba, Ibaraki 305-0047, Japan*
[2]*Graduate school of Science and Technology, Niigata University, 8050, Ikarashi 2-no-cho, Nishi-ku, Niigata, 950-2181, Japan*
[3]*Faculty of Science, Niigata University, 8050, Ikarashi 2-no-cho, Nishi-ku, Niigata, 950-2181, Japan*
[4]*Faculty of Science, University of the Ryukyus, Nishihara, Okinawa 903-0213, Japan*
(Received 21 December 2011; published 27 February 2012)

We report on comprehensive measurements of the magnetic, transport, and thermal properties of the Heusler type compound $Fe_{2+x}V_{1-x}Al$ at $-0.05 \leqslant x \leqslant 020$. We show that while stoichiometric Fe_2VAl is a nonmagnetic semimetal (or narrow-gap semiconductor), a substitution on the nominal V-sites with the Fe atom leads to a ferromagnetic ground state above $x = x_c$ (∼0.05) with a rising Curie temperature T_C and an ordered moment M_s. At $x = 0.1$ and 0.2, the reduced value of the ratio $M_s/P_{eff} \ll 1$, where P_{eff} is the effective Curie-Weiss moment, together with the analysis of the magnetization data $M(H,T)$, shows magnetism is itinerant. At a higher temperature $T \sim 60$ K, a Schottky anomaly in specific heat C is indicated prominently at $x > 0$, while the anomaly is observable in the whole experimental range of x. At a lower temperature, an electronic component $\Delta C/T$ in specific heat shows a divergence that arises at both $x < 0$ and $x > 0$. The resistivity–temperature curve $\rho(T)$ in the vicinity of the ferromagnetic quantum critical point, $x \sim 0.05$, shows a non-Fermi liquid behavior, $\rho \sim T^n$ ($n \sim 1$), above $H > 20$ kOe.

DOI: 10.1103/PhysRevB.85.085130 PACS number(s): 75.30.Kz, 75.47.−m, 71.20.Be

I. INTRODUCTION

The Heusler type iron–vanadium compound Fe_2VAl and related alloys have attracted considerable attention[1–6] since it was claimed that these $3d$-electron systems with small carrier concentration, $n \approx 0.01$ per formula unit (f.u.),[2] exhibit significant carrier mass[1] and thermoelectric[6–8] enhancements and non-Fermi liquid (NFL) behavior.[1] Stoichiometric Fe_2VAl is nonmagnetic, and related alloys, such as $Fe_{2+x}V_{1-x}Al$ and $Fe_2VAl_{1-\delta}$, exhibit ferromagnetic transitions.[2,5,6,9–11] Consequently, the samples at $x \approx 0$ and $\delta \approx 0$ are located at the brink of the ferromagnetic order, close to the ferromagnetic quantum critical point (QCP), i.e., $T_C \rightarrow 0$.[1,3] Stimulated by these findings, theoretical work claimed Fe_2VAl is a nonmagnetic semimetal with the pseudogap (∼0.5 eV, hereafter denoted as a large pseudogap) at the Fermi level.[12–14] The considerable mass enhancement of the conduction carriers was attributed to excitonic correlations[13] or spin fluctuations.[12,14] However, subsequent specific heat $C(T)$ measurements in applied magnetic fields showed that the upturn in C/T at low temperatures results from a Schottky contribution of paramagnetic clusters in Fe_2VAl,[3] while at the zero field, the low-temperature upturn[1,3,15] and a round maximum at T of ∼0.4 K[16] in C/T were observed. It is still an open question as to where the ferromagnetic QCP is and whether the anomalous temperature dependence in C/T is accompanied with the proximity to the QCP, because there are crystallographic disorders, e.g., the antisite defects and off-stoichiometry in the Heusler type Fe_2VAl and the related compounds, that strongly affect physical quantities.[1,2] Comprehensive studies are needed to reveal the quantum criticality and the effects of the disorder by using nominal off-stoichiometric samples such as $Fe_{2+x}V_{1-x}Al$ or $Fe_2VAl_{1-\delta}$, which can introduce magnetic clusters at x and $\delta > 0$, respectively. In this paper, we investigate bulk properties, e.g., electric resistivity, magnetization, and specific heat, under a magnetic field for $-0.05 \leqslant x \leqslant 0.20$ in $Fe_{2+x}V_{1-x}Al$. As indicated recently in a semimetallic $Fe_2VAl_{0.95}$,[17] exhibiting a bulk ferromagnetism with a Curie point of $T_C = 33$ K, in $Fe_{2+x}V_{1-x}Al$ a ferromagnetism emerges at $x > x_c$ (∼0.05) with itinerant electron characteristics. Specific heat $C(T)$ measurements reveal that there is a small pseudogap with $\Delta \sim 100$ K at the Fermi level, while the low-temperature C/T and magnetoresistance are enhanced strongly at $x \sim 0.05$, where the Curie point and ordered moment vanish.

II. EXPERIMENTAL DETAILS

Polycrystalline samples of $Fe_{2+x}V_{1-x}Al$ were prepared by arc melting the proper amounts of the elements into the nominal chemical composition. The samples were subjected to a heat treatment at 1000 °C for 15 h for homogenization purposes and then annealed at 400 °C for 15 h. For all samples, the crystal structure was identified as the Heusler type. No secondary phases were detected in the powder x-ray diffraction (XRD) profiles. After annealing the grain size (i.e., the individual crystallite size) in the polycrystalline samples is quite large (more than several hundredths of a micrometer), so we expect the volume fraction of impurity phases located at the grain boundaries to be quite low. The samples we report on in this work are the same as those previously characterized by XRD, scanning electron microscopy, and energy dispersive x-ray spectroscopy.[2,6,17] Static magnetization, specific heat, and resistivity measurements down to $T = 2$ K were carried out using a conventional superconducting quantum interference device magnetometer (MPMS-XL, Quantum Design), a conventional physical property measurement system (PPMS, Quantum Design) with an alternative current (AC) transport and a heat capacity options, respectively. Low-temperature resistivity measurements down to $T = 0.23$ K were carried out in a ^3He refrigerator (Heliox VL, Oxford Instruments) with a sensitive

LR700 (Linear Research) AC-resistance bridge at the Van der Waals-Zeeman Institute of the University of Amsterdam.

III. RESULTS AND DISCUSSIONS

Figure 1(a) shows the magnetization of $x = 0.1$ and 0.2 in $Fe_{2+x}V_{1-x}Al$ as a function of the magnetic field $M(H)$ measured at $T = 2$ K. The saturation moment M_s of $x = 0.1$ and 0.2 at $T = 2$ K can be estimated to be 0.37 and 0.74 μ_B/f.u., respectively, from an extrapolation of the $M(H)$ versus $1/H$ plot to $1/H \to 0$. For $x = 0.1$ and 0.2, a small ferromagnetic component M_0 in magnetization can be observed even in the paramagnetic temperature region ($T > T_C$). We traced the temperature variation of M_0 obtained from M-H curves, which can be expressed as $M = M_0 + \chi H$ above $H = 2$ kOe (data not shown), and the corrected magnetization, which can be expressed as $M_{cor} = M - M_0$ at $H = 50$ kOe. As indicated in Fig. 1(b) by the straight line in the plot of H/M_{cor} $(= 1/\chi)$ versus T, the susceptibility follows a Curie-Weiss law, $\chi(T) = C/(T - \theta)$, for $T > 100$ K, from which we extract the Curie constant $C = 0.71$ emuK/mol and a Curie-Weiss temperature $\theta = 43$ K. By using $C = N{p_{eff}}^2{\mu_B}^2/3k_B$, an effective magnetic moment $p_{eff} = 2.38$ μ_B/f.u. is obtained, where N, μ_B, and k_B are the number of the ($Fe_{2.1}V_{0.9}Al$) formula unit, the Bohr magneton, and Boltzmann's constant, respectively. The saturation moment at $T = 2$ K is $M_s = 0.37$ μ_B/f.u., which is much smaller than the paramagnetic moment $p_{eff} = 2.38$ μ_B/f.u. The small value of the ratio $M_s/p_{eff} = 0.15$ corroborates the itinerant electron nature of ferromagnetism in $Fe_{2.1}V_{0.9}Al$. The ferromagnetic transition in $Fe_{2.1}V_{0.9}Al$ is also signaled (data not shown here): (1) in the temperature derivative of the resistivity $d\rho/dT$, (2) by the $M^4 - M/H$ plot, and (3) by the $M^2 - (T/T_C)^2$ and $M^2 - (T/T_C)^{4/3}$ plots. The transition temperatures $T_C = 15 \pm 2$ K determined by the different techniques agree within the uncertainty of 2 K, whereas the temperature variation of the specific heat divided by temperature, C/T, showed no lambda-shaped anomaly (Fig. 3(b), as discussed later). In Fig. 1(c) and (d), we analyze the magnetization data around T_C in terms of $M^4 - H/M$ plots for $x = 0.10$ and 0.20, respectively. For weak ferromagnetic systems, the M^4 versus H/M curve at $T = T_C$ is predicted to be linear with an intercept zero.[18] Inspecting Fig. 1(d), we conclude that $T_C = 15$ K. However, in the Arrott plot, the M^2 versus H/M curves all exhibit a strong curvature toward the H/M axis. These features are quite similar to those found in prototypical itinerant ferromagnets, like MnSi and Ni_3Al.[18] For $x = 0.20$, magnetic transition occurs at $T_C = 65 \pm 3$ K with $M_s = 0.74$ and $p_{eff} = 4.75$ μ_B/f.u. ($M_s/p_{eff} = 0.15$). In addition, the magnetic data for $x = 0.20$ provide strong evidence for itinerant ferromagnetism [see also Fig. 1(d)].

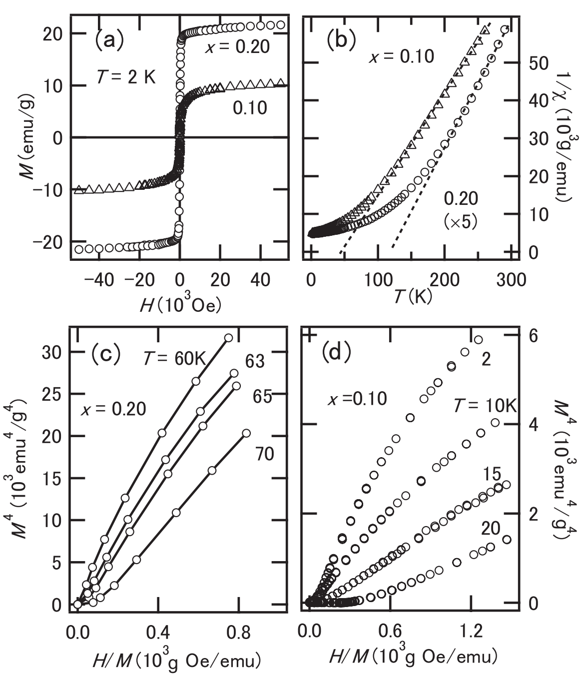

FIG. 1. (a) Magnetization as a function magnetic field ($M - H$ curves) of $x = 0.10$ and 0.20 in $Fe_{2+x}V_{1-x}Al$ at $T = 2$ K. (b) Temperature dependence of reciprocal susceptibility $1/\chi$ for $x = 0.10$ and 0.20. (c) and (d) $M^4 - H/M$ curves at constant temperatures as indicated for $x = 0.20$ and 0.10, respectively.

In contrast, for $x = 0.05$, no ferromagnetic transition occurs, at least down to $T = 2$ K. As indicated in the inset of Fig. 2(b), the $M^2 - H/M$ (Arrott) plot for $x = 0.05$ does not intercept zero at $T \geqslant 2$ K; that is, $T_C < 2$ K. Contrary to the case of $x \geqslant 0.10$, the $M^4 - H/M$ plot for $x = 0.05$ has a strong curvature toward the M^4 axis. From the observed x-variations of T_C [Fig. 2(a)] and M_s [Fig. 2(b)] determined by the measurements of several quantities below $x = 0.20$, we can deduce that both T_C and M_s emerge at $x \sim 0.05$. Similar to the quantum critical behaviors observed in the heavy fermion system, e.g., $URh_{1-x}Ru_xGe$[19] and $CePd_{1-x}Rh_x$[20] in the vicinity of ferromagnetic QCP, low-temperature C/T is enhanced at $x_c \sim 0.05$ in $Fe_{2+x}V_{1-x}Al$ [Figs. 3(b) and 4(a)]. These findings might derive a plausible interpretation to the mechanism for

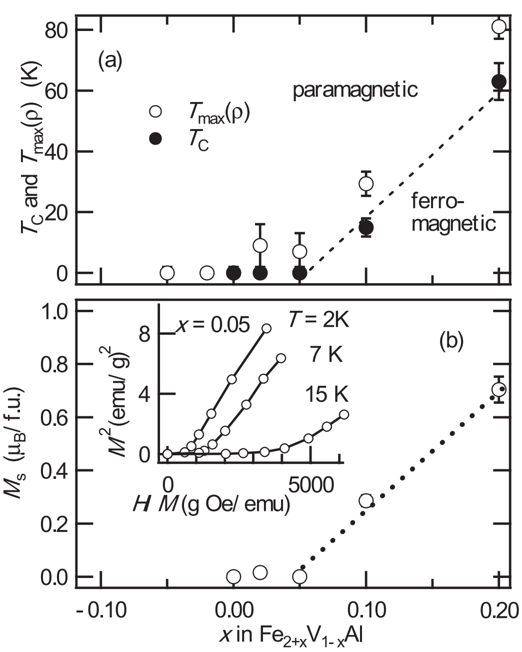

FIG. 2. (a) Curie point, T_C, and $T_{max}(\rho)$ as functions of x. (b) M_s at $T = 2$ K obtained by this work as a function of x. Dashed lines are visual guides. The inset shows the Arrott plot for $x = 0.05$.

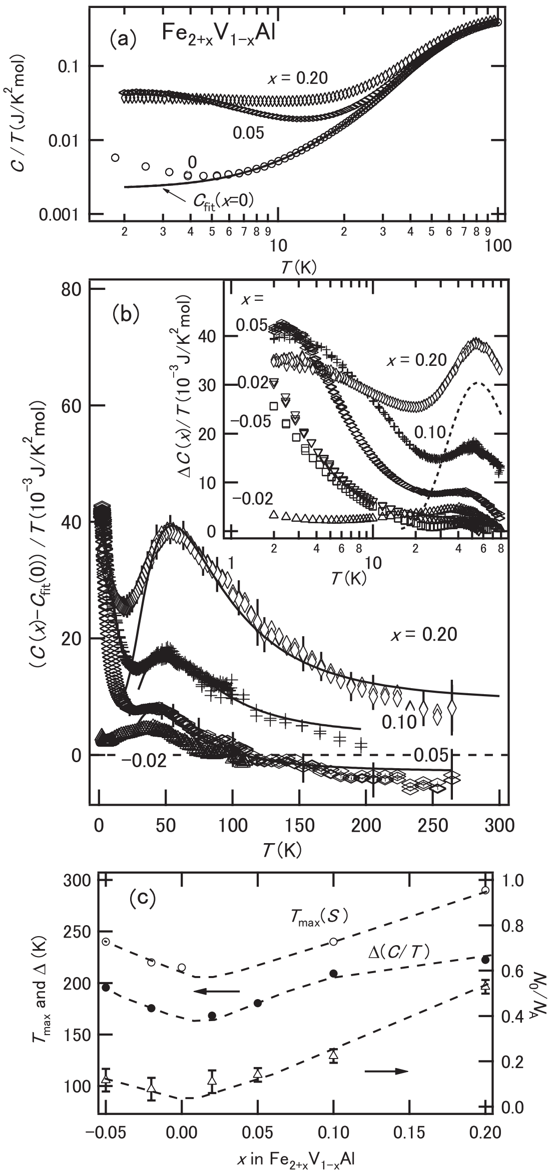

FIG. 3. (a) Specific heat divided by temperature $C(x)/T$ plotted as a function of T of $Fe_{2+x}V_{1-x}Al$ in a zero magnetic field. The solid curve $C_{\text{fit}}(T)$ represents the fit to $C(x=0)/T$ in the temperature region 8 K $< T <$ 30 K. (b) Temperature dependence of $\Delta C/T = [C(x) - C_{\text{fit}}(x=0)]/T$ for $x = -0.02$, 0.05, 0.10, and 0.20. Solid lines are fits by the Schottky specific heat with a residual T-linear term. The inset shows $\Delta C/T$ versus logarithmic temperature plot below 80 K. The dashed curve represents the Schottky component for $x = 0.20$. (c) Δ and N_0/N_A as functions of x. For comparison, the maximum temperature $T_{\max}(S)$ in the Seebeck coefficient (Ref. 6) is shown.

the low-temperature upturn in C/T, that is, proximity to a ferromagnetic QCP located at $x = x_c$ slightly higher than $x = 0$. A low-temperature upturn has been observed in Fe_2VAl[1,3] and in $Fe_{2+x}V_{1-x}Al$ for $-0.08 \leqslant x \leqslant 0.01$.[21,22] As indicated in Fig. 3(a), the difference in specific heat between $x = 0$ and $x \neq 0$ is remarkable in the low-temperature region. Employing paramagnetic Fe_2VAl as a reference material in the specific heat,[3,17] a compositional change defined as $\Delta C/T = [C(x) - C_{\text{fit}}(Fe_2VAl)]/T$ at the zero field is obtained as shown in Fig. 3(b), where $C_{\text{fit}}(x)$ is a numerically fitted specific heat curve above 8 K. No clear anomaly is presented at T_C, since the ordered magnetic moment ($M_s = 0.37\ \mu_B$/f.u.), and hence the corresponding magnetic entropy, seems to be quite small. For the weak ferromagnet $Fe_2VAl_{0.95}$ ($T_C = 33$ K and $M_s = 0.24\ \mu_B$/f.u.) exhibiting a weak lambda-type anomaly in specific heat, it was estimated to be quite a small value: 0.7% of $R\ln 2$ at $T = T_C$, where R is the gas constant.[17]

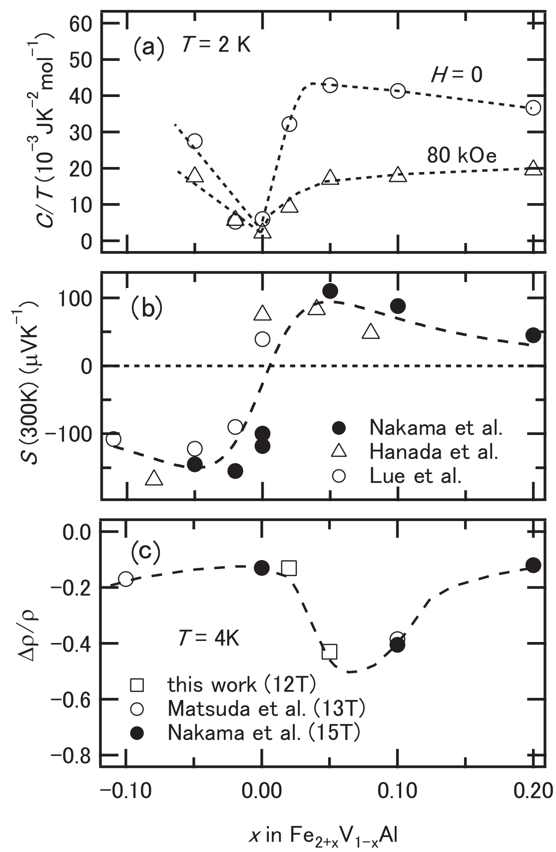

FIG. 4. (a) C/T ($T = 2$ K) at $H = 0$ and 80 kOe as a function of x in $Fe_{2+x}V_{1-x}Al$. (b) Seebeck coefficient at 300 K as a function of x as reported previously (Refs. 6–8). (c) Magnetoresistance ratio $[\rho(H) - \rho(0)]/\rho(0)$ at 4 K as a function of x as reported previously (Refs. 4 and 6) and in this work. All dashed lines are the visual guides.

As indicated in Fig. 3(b), there are two distinct features in the vicinity of x_c: (1) the electronic specific heat component is enhanced and $\Delta C/T$ increases with decreasing temperature in the lower-temperature region and (2) a Schottky-like peak is indicated at T of $\sim$50–60 K. Both develop with increasing and decreasing x from $x = 0$. We tried to fit $\Delta C/T$ in the range of $20 < T < 100$ K to the two-level system with a residual electronic component, $\Delta C = \gamma_{\text{res}}T + N_0\nu(\Delta/T)^2\exp(-\Delta/T)/[1 + \nu\exp(-\Delta/T)]^2$ [Fig. 3(b)], where γ_{res}, N_0, ν, and Δ are the residual T-linear coefficient, a numerical fitting constant, the degeneracy ratio of excited and ground states ($= g_0/g_e$), and an energy splitting ($= \varepsilon_e - \varepsilon_0$), respectively [Fig. 3(c)]. We assumed $\nu = 1$. At $x > 0$, the number of the Schottky center $N_0/N_A \sim 3x$, where N_A is Avogadro's constant, corresponds to the number of doped valence electrons in $Fe_{2+x}V_{1-x}Al$. This suggests that the Fe atoms substituted into the Fe_I sites lead to the appearance of peaks of density of states (DOS) around ε_F, considerably modifying the DOS structure. As indicated in the Kondo insulators and speculated recently in $Fe_2VAl_{0.95}$, a complicated DOS structure, e.g., the V-shaped DOS with a small residual component at the Fermi level, is expected in $Fe_{2+x}V_{1-x}Al$.[14] Using the *ab initio* method, Deniszczyk obtained magnetic and paramagnetic band structures of $Fe_{2+x}V_{1-x}M$ (M = Al and Ga) in the range of $0.0625 \leqslant x \leqslant 0.50$[23] and indicated in the large pseudogap (~0.5 eV) the sharp structure of DOS around ε_F, consisting of the $3d$-state of the Fe atoms at the Fe_I-site and developing with increasing x. Expectedly, the glowing sharp DOS with increasing x can reflect the temperature dependences on ρ. Assuming temperature dependence of $\rho(T) = \rho_0 \exp(\Delta_r/2T)$ in $150 > T > 300$ K, we confirmed $\Delta_r = 190$ K $\sim\Delta$ at $x > 0$, whereas $\Delta_r \sim 1000$ K is estimated in a higher temperature of $300 > T > 800$ K.[6]

However, at the lower temperature, $\Delta C/T$ at $x < 0.05$ exhibits a divergence with a power law $\sim T^{-\alpha}$ down to 2 K [Fig. 3(b)]. This might be a signal that a NFL state emerged coincidently where a ferromagnetic quantum transition taking place, $x \sim 0.05$. Generally, NFL behavior is characterized by a power law or logarithmic temperature dependence in C/T and χ. Also, the quadratic temperature variation in resistivity, $\rho - \rho_0 \sim T^2$, which is one of the characteristics of Fermi liquids, is deviated to $\sim T^n$ with $n < 2$, where ρ_0 is the residual resistivity. In rare earths and actinide metallic compounds, the competition between magnetic and Kondo interactions seems to be relevant for the physics of the quantum critical transition from the magnetically ordered to the paramagnetic state at $T = 0$. The localized magnetic moments in the paramagnetic state are quenched by the Kondo effect with conduction electron spins, while in the magnetically ordered state, the localized moments establish a long-range magnetic order by the Ruderman-Kittel-Kasuya-Yosida interaction, which is mediated by conduction spins. The NFL behavior is observed often at the paramagnetic state close to the QCP. Theoretical models as possible explanations for the NFL behavior based on a single impurity model and proximity to a QCP have been proposed. However, to establish the system to be at the QCP, we can tune the electronic state by the substitution of elements in the compounds. This common procedure introduces disorders into the system. It was predicted theoretically that disorders can play a significant role in the deviation from the Fermi liquid characteristics in the vicinity of a QCP in f-electron alloys. The Kondo lattice model with disorder and magnetic anisotropy leads to the coexistence of a metallic paramagnetic state with a granular magnetic state.[24] This coexistence phase is equivalent to the Griffiths phase of dilute magnetic systems. The thermodynamic properties are predicted to follow the power law behavior, $C/T \sim \chi \sim T^{-1+\lambda}$, with a nonuniversal exponent of $0 < \lambda < 1$. Even in transition metal compounds, e.g., $Cr_{1-x}V_x$, MnSi, and $ZrZn_2$, which do not contain rare earths or actinide element, a NFL behavior has been indicated.[25] Recently, it was reported that the Heusler type Fe_2VGa,[26] $Fe_2V_{1-x}Ti_xGa$, and $Fe_2V_{1-x}Rh_xGa$[27] exhibit low-temperature divergences in C/T and χ, while the stoichiometric compound has been predicted by band calculations to be semimetals with small a pseudogap in the DOS at the Fermi level (Ref. 26) or narrow-gap semiconductors.[27] The antisite defects between the Fe_I and the Fe_{II} sites seem to be the main sources for magnetic clusters with a magnetic moment of $\sim 3.7\ \mu_B$ and attribute the divergence at a lower temperature $C/T \sim \chi \sim T^{-\alpha}$ with $\alpha \sim 0.3$ in a stoichiometric Fe_2VGa.[26] A small ferromagnetic component is observed at $-0.05 \leqslant x \leqslant 0.10$, M_{sp}, ~0.2–2 × 10^{-2} emu/g (data not shown here); therefore, we can deduce that the Griffiths phase is also realized in $Fe_{2+x}V_{1-x}Al$ and demonstrate evidence for the Griffiths phase. For the ferromagnet of $x = 0.10$, susceptibility can be fitted well to $\chi \propto (T - T_G)^{-1+\lambda}$ with a nonuniversal exponent $\lambda = 0.27$ and $T_G = 19.7$ K slightly larger than T_C obtained in this work [Fig. 5(a)]. As obtained theoretically,[28] the M-H curve is also represented by $M \sim H^{\lambda}$ with $\lambda = 0.16$ [Fig. 5(b)] at a temperature slightly higher than T_C. It was theoretically obtained by Neto *et al.*[28] that the low-temperature divergence is strongest at the QCP ($\lambda = 0$) and the Fermi liquid characteristics ($\lambda = 1$) are established far from the QCP. Although it would be still controversial whether the C/T upturn at the zero field is due to a distribution of magnetic anisotropies in paramagnetic clusters[3] or due to proximity to the ferromagnetic QCP,[26] our data resemble those of Guo *et al.* (Co-doped FeS_2)[29] and Ślebarski *et al.* (disordered Fe_2VGa),[26,27] who claim to find evidence for Griffiths phases.

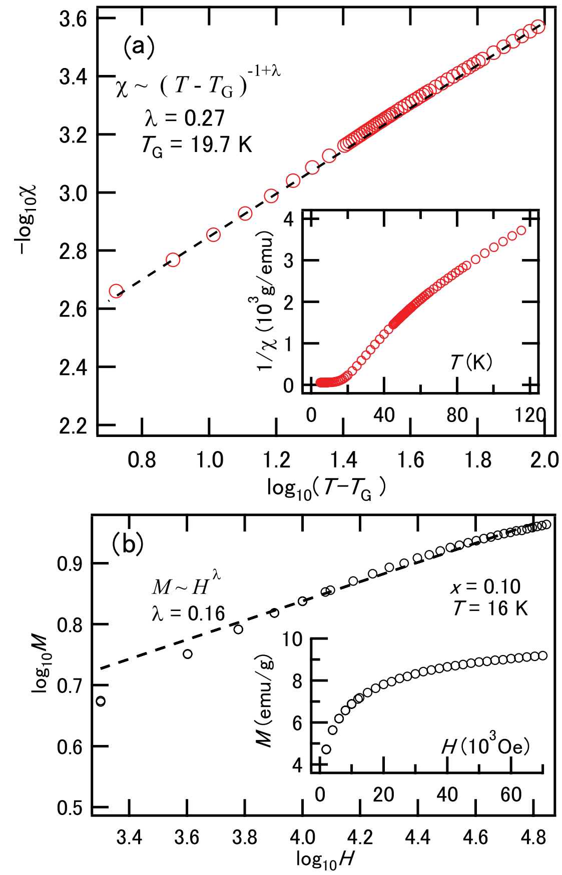

FIG. 5. (Color online) (a) Logarithmic plot of $\chi(H = 200$ Oe) versus $T - T_G$ at $x = 0.10$. The dashed line represents the fitted line to $\chi \sim (T - T_G)^{-1+\lambda}$. The inset shows a temperature dependence of reciprocal susceptibility measured. (b) Logarithmic plot of $M(T = 16$ K) versus H for $x = 0.10$. The dashed line represents the fitted line to $M \sim H^{\lambda}$. The inset shows the field dependence of magnetization.

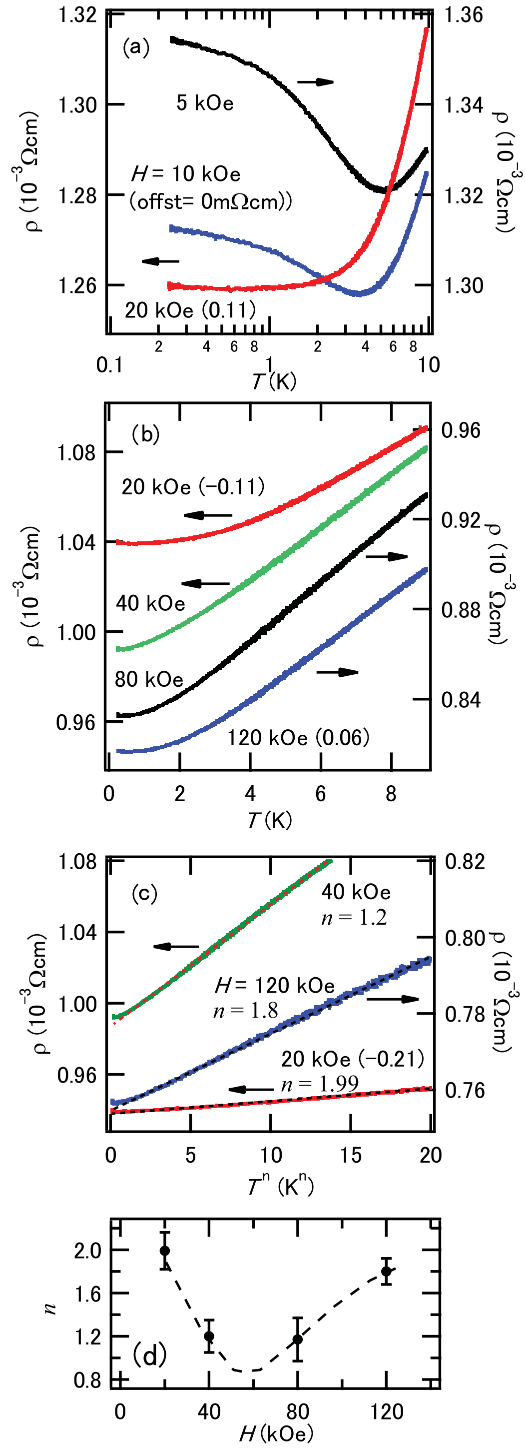

FIG. 6. (Color online) (a) Semilogarithmic plot of resistivity $\rho(T)$ at $H = 5$, 10, and 20 kOe in $Fe_{2.05}V_{0.95}Al$. The parenthetic values are the vertical offsets. (b) $\rho(T)$ curves at $H = 20$, 40, 80, and 120 kOe below 9 K. (c) Resistivity as a function of T^n at $H = 20$, 40, and 120 kOe. The estimated exponent n is indicated by the curve. (d) Field dependence on the exponent n. All dashed lines and curve are visual guides.

Actually, at $x = 0.05$ resistivity, $\rho(T)$ shows NFL behavior: $\rho - \rho_0 = A'T^n$, with $n < 2$ as shown in Fig. 6(c). From a lower magnetic field, $\rho(T)$ exhibits a minimum shifting toward a lower temperature with an increasing magnetic field, which reveals the existence of a Kondo effect or the effect of the crystallographic disorder at a lower temperature [Fig. 6(a)]. The exponent n obtained in the field-induced metallic state above $H = 20$ kOe shows an obvious deviation from $n = 2.0$ and makes a minimum ($n \sim 1$) at $H \sim 60$ kOe [Fig. 6(d)]. At a higher magnetic field of $H > 120$ kOe, n seems to recover to that of the Fermi liquid state ($n = 2$). This resembles the system that is tuned by an external magnetic field, pushing the system from the paramagnetic to the ferromagnetic state. These findings in $\rho(T)$ under a magnetic field are consistent with the speculation that the QCP locates in the vicinity of $x = 0.05$ in $Fe_{2+x}V_{1-x}Al$. We could not rule out the possibility, originally claimed by Nishino *et al.*,[1] that the divergence in specific heat observed in stoichiometric Fe_2VAl samples[1,3,16] is the NFL behavior due to the proximity to the ferromagnetic QCP, whereas the QCP is plausibly at $x \sim 0.05$ but not at $x = 0$.

As mentioned previously, the ferromagnetic state at $x = 0.10$ and 0.20 has an itinerant nature; consequently, localized electronic spins in the magnetic cluster are facilitated to be delocalized and to participate in the long-range ferromagnetic order with increasing x. This scenario is supported by the band calculations.[30,31] The situation that the narrow $3d$-band locates in the vicinity of ε_F originated from the Fe atoms in the Fe_I-site surrounded by eight Fe atoms at the Fe_{II} site (the so-called $^{\beta}$Fe, denoted after Deniszczyk) resembles that of the heavy fermion f-electron system.[30,31] For $x < x_c$, the $^{\beta}$Fe-spin is isolated and behaves as a localized spin, interacting solely with conduction electrons. With increasing x, the $^{\beta}$Fe-electrons interact with one another via the hybridization with conduction electrons. Then, long-range magnetic ordering is established above x_c. For $x = 0.10$ and 0.20, the quadratic temperature dependence in resistivity is indicated below T_C, while a weak upturn, probably due to VRH conduction[4] or Kondo scattering,[16] is realized at a lower temperature. For $x = 0.20$, from obtained large quantities of $A = 0.12\ \mu\Omega\mathrm{cmK}^{-2}$ and $\gamma \sim 30$–40 $\mathrm{mJK^{-2}mol^{-1}}$, we derive $A/\gamma^2 \sim 1 \times 10^{-4}\ \Omega\mathrm{cmJ^{-2}K^2mol^2}$—much larger than the Kadowaki-Woods constant, $1 \times 10^{-5}\ \Omega\mathrm{cmJ^{-2}K^2mol^2}$. The large deviation in A/γ^2 seems to be due to a small carrier number, $n_c \ll 1$, since A/γ^2 is proportional to k_F^{-4} ($\propto n_c{}^{-4/3}$).[32] Plausibly, the large mass enhancement is realized by delocalizing the narrow band $^{\beta}$Fe-electrons even in the ferromagnetic state with a small carrier concentration, $n_c \sim 0.2$.

As shown in Fig. 4(b), the Seebeck coefficient S exhibits the maximum and the minimum at $x \sim \pm 0.05$, respectively. While the large pseudogap of ~5000 K is formed with a residual small DOS $N(\varepsilon_F)$ at ε_F[12–14] for the stoichiometric Fe_2VAl, once the $^{\beta}$Fe electrons are introduced, along with an analogue to the enhancement of S in the Kondo insulator,[1,33] the small pseudogap is established at $\varepsilon \sim \varepsilon_F$. When ε_F situates at one of the sharp edges separated from another with Δ in energy, S is strongly enhanced, because $S \propto \mathrm{d}\ln N(\varepsilon_F)/\mathrm{d}\varepsilon$ at $T < \Delta$.[34] However, $|S|$ makes a maximum at $T \sim \Delta$ and decreases with increasing temperature at $T > \Delta$, because the opposite charges, excited thermally, contribute to the thermoelectric power.[6] Actually, the x-dependence of the maximum and minimum temperatures T_{max} and T_{min}, respectively, in Seebeck coefficient[6] is traced well with that of Δ [Fig. 3(c)]. This scenario is somewhat similar to the case of the Tl-doped

PbTe,[35] showing an excellent thermoelectric figure of merit $zT > 1$ at $T > 600$ K.[35] In a classical thermoelectric semiconductor PbTe, Tl creates additional energy levels, sometimes called resonant levels, in the valence band and brings the increment of the effective mass ratio m^*/m by a factor of ~ 3 in $Tl_{0.015}Pb_{0.985}Te$.[35] Recently, first principle calculations showed that in Fe_2VAl, the antisite defects introduce d-states in the gap (localized in-gap states) and the resonant states close to the gap region with a magnetic moment of ~ 4 μ_B/defect.[31] In $Fe_{2+x}V_{1-x}Al$, S is strongly enhanced, at which $\Delta C/T$ exhibits the strong divergence; i.e., the Griffiths phase (coexistence of conduction electrons with localized magnetic clusters) seems to be realized at both $x > 0$ and $x < 0$ [Fig. 4(a) and 4(b)]. In contrast, the giant magnetoresistance (GMR) is significant at $x > 0$ but not at $x < 0$ [Fig. 4(c)]. This is reminiscent of a claim that the GMR is the quantum Griffiths singularity in perovskite manganite.[36] As mentioned previously, residual entropy due to undercompensated cluster spins might play a significant role for the anomalous behaviors in thermodynamic and magnetic quantities in the Heusler type iron compounds Fe_2VAl, Fe_2VGa, and their related alloys.

IV. CONCLUSIONS

Magnetic, transport, and specific heat measurements have been carried out on the Heusler type compound $Fe_{2+x}V_{1-x}Al$ in $-0.05 \leqslant x \leqslant 0.20$. The data reveal a ferromagnetic quantum transition, which takes place at $x_c \sim 0.05$, and thermal transitions at $T_C = 15$ and 63 K for $x = 0.10$ and 0.20, respectively. While the magnetism has the typical characteristics of a weak itinerant ferromagnet, the deviations from the Fermi liquid characteristics (NFL behaviors) in magnetization, specific heat, and resistivity are indicated at $x \sim x_c$. With increasing x, a Schottky anomaly in specific heat develops with the energy gap $\Delta \sim 150$ K and a residual T-linear term in specific heat.

ACKNOWLEDGMENTS

T. N. appreciates K. Matsubayashi (Institute for Solid State Physics, University of Tokyo) for valuable discussions and A. de Visser (Van der Waals-Zeeman Institute, University of Amsterdam) for providing an excellent cryogenic measurement system.

*naka.takashi@nims.go.jp

[1] Y. Nishino, M. Kato, S. Asano, K. Soda, M. Hayasaki, and U. Mizutani, Phys. Rev. Lett. **79**, 1909 (1997).
[2] A. Matsushita, T. Naka, Y. Takano, T. Takeuchi, T. Shishido, and Y. Yamada, Phys. Rev. B **65**, 075204 (2002).
[3] C. S. Lue, J. H. Ross, C. F. Chang, and H. D. Yang, Phys. Rev. B **60**, R13941 (1999).
[4] H. Matsuda, K. Endo, K. Ooiwa, and M. Iijima, J. Phys. Soc. Jpn. **69**, 1004 (2000).
[5] K. Soda, H. Murayama, K. Shimba, S. Yagi, J. Yuhara, T. Takeuchi, U. Mizutani, H. Sumi, M. Kato, H. Kato, Y. Nishino, A. Sekiyama, S. Suga, T. Matsushita, and Y. Saitoh, Phys. Rev. B **71**, 245112 (2005).
[6] T. Nakama, Y. Takaesu, K. Yagasaki, T. Naka, A. Matsushita, K. Fukuda, and Y. Yamada, J. Phys. Soc. Jpn. **74**, 1378 (2005).
[7] Y. Hanada, R. O. Suzuki, and K. Ono, J. Alloy. Compd. **329**, 63 (2001).
[8] C. S. Lue and Y.-K. Kuo, Phys. Rev. B **66**, 085121 (2002).
[9] Y. Nishino, Mater. Trans. JIM **42**, 902 (2001).
[10] Y. Nishino, C. Kumada, and S. Asano, Scr. Mater. **36**, 461 (1997).
[11] T. Naka, T. Adschiri, K. Fukuda, F. Ishikawa, Y. Yamada, Y. Takaesu, T. Nakama, K. Yagasaki, and A. Matsushita, J. Magn. Magn. Mater. **310**, 1059 (2007).
[12] D. J. Singh and I. I. Mazin, Phys. Rev. B **57**, 14352 (1998).
[13] R. Weht and W. E. Pickett, Phys. Rev. B **58**, 6855 (1998).
[14] G. Y. Guo, G. A. Bottonz, and Y. Nishino, J. Phys. Condens. Matter **10**, L119 (1998).
[15] A. Matsushita and Y. Yamada, J. Magn. Magn. Mater. **196-197**, 669 (1999).
[16] S. Nishigori, Y. Yamada, T. Ito, H. Abe, and A. Matsushita, Phys. B **281-282**, 686 (2000).
[17] K. Sato, T. Naka, M. Taguchi, T. Nakane, F. Ishikawa, Y. Yamada, Y. Takaesu, T. Nakama, A. de Visser, and A. Matsushita, Phys. Rev. B **82**, 104408 (2010).
[18] Y. Takahashi, J. Phys. Soc. Jpn. **55**, 3553 (1986).
[19] N. T. Huy, A. Gasparini, J. C. P. Klaasse, A. de Visser, S. Sakarya, and N. H. van Dijk, Phys. Rev. B **75**, 212405 (2007).
[20] T. Westerkamp, M. Deppe, R. Küchler, M. Brando, C. Geibel, P. Gegenwart, A. P. Pikul, and F. Steglich, Phys. Rev. Lett. **102**, 206404 (2009).
[21] Y. Nishino, Intermetallics **8**, 1233 (2000).
[22] Y. Nishino, H. Sumi, and U. Mizutani, Phys. Rev. B **71**, 094425 (2005).
[23] J. Deniszczyk, Acta Phys. Pol. B **32**, 529 (2001).
[24] A. H. C. Neto, G. Castilla, and B. A. Jones, Phys. Rev. Lett. **81**, 3531 (1998).
[25] H. Löhneysen, A. Rosch, M. Vojta, and P. Wölfle, Rev. Mod. Phys. **79**, 1015 (2007).
[26] A. Ślebarski and J. Goraus, Phys. Rev. B **80**, 235121 (2009).
[27] A. Ślebarski, J. Goraus, and M. Fijałkowski, Phys. Rev. B **84**, 075154 (2011).
[28] A. H. C. Neto and B. A. Jones, Europhys. Lett. **71**, 790 (2005).
[29] S. Guo, D. P. Young, R. T. Macaluso, D. A. Browne, N. L. Henderson, J. Y. Chan, L. L. Henry, and J. F. DiTusa, Phys. Rev. Lett. **100**, 017209 (2008).
[30] J. Deniszczyk and W. Borgiel, Acta Phys. Pol. B **34**, 1257 (2003).
[31] D. I. Bilc and P. Ghosez, Phys. Rev. B **83**, 205204 (2011).
[32] K. Yamada, *Electron Correlation in Metals* (Cambridge University Press, Cambridge, United Kingdom, 2004), Chap. 7, p. 127.
[33] I. Terasaki, I. Tsukada, and Y. Iguchi, Phys. Rev. B **65**, 195106 (2002).
[34] N. F. Mott and H. Jones, *The Theory of the Properties of Metals* (Clarendon Press, Oxford, 1936).
[35] J. P. Heremans, V. Jovovic, E. S. Toberer, A. Saramat, K. Kurosaki, A. Charoenphakdee, S. Yamanaka, and G. J. Snyder, Science **321**, 554 (2008).
[36] M. B. Salamon, P. Lin, and S. H. Chun, Phys. Rev. Lett. **88**, 197203 (2002).